Formation and evolution of galaxy outskirts
Proceedings IAU Symposium No. 321, 2015
Armando Gil de Paz, Johan Knapen & Janice Lee

DOI: 00.0000/X000000000000000X

Properties of the outer regions of spiral disks: abundances, colors and ages

Mercedes Mollá[1], Angeles I. Díaz[2,3], Brad K. Gibson[4], Oscar Cavichia[5], and Ángel-R. López-Sánchez[6,7]

[1]Departamento de Investigación Básica, CIEMAT, 28040, Madrid. Spain
email: mercedes.molla@ciemat.es
[2] Universidad Autónoma de Madrid, 28049, Madrid, Spain
[3] Astro-UAM, Unidad Asociada CSIC, Universidad Autónoma de Madrid, 28049, Madrid, Spain
[4] E.A. Milne Centre for Astrophysics, Dept. of Physics & Mathematics, University of Hull, Hull, HU6 7RX, United Kingdom
[5] Instituto de Física e Química, Universidade Federal de Itajubá, Av. BPS, 1303, 37500-903, Itajubá-MG, Brazil
[6]Australian Astronomical Observatory, PO Box 915, North Ryde, NSW 1670, Australia
[7]Department of Physics and Astronomy, Macquarie University, NSW 2109, Australia

Abstract. We summarize the results obtained from our suite of chemical evolution models for spiral disks, computed for different total masses and star formation efficiencies. Once the gas, stars and star formation radial distributions are reproduced, we analyze the Oxygen abundances radial profiles for gas and stars, in addition to stellar averaged ages and global metallicity. We examine scenarios for the potential origin of the apparent flattening of abundance gradients in the outskirts of disk galaxies, in particular the role of molecular gas formation prescriptions.

Keywords. Galaxy: abundances; Galaxy: evolution; galaxies: abundances; ISM: abundances

1. Introduction

Chemical evolution models are the classical tool by which to interpret observed elemental abundances, and associated quantities such as gas and stellar surface densities, star formation histories, and the distribution of stellar ages. Elemental patterns carry the fingerprint of star formation timescales from their birth location, regardless of a star's present-day position. Chemical evolution codes solve a system of first order integro-differential equations, assuming an analytical star formation (SF) law, initial mass function (IMF), stellar lifetimes, and nucleosynthetic yields.

In Mollá & Díaz (2005), we calculated a grid of 440 theoretical galaxy models, (44 radial mass distributions, and 10 molecular gas and SF efficiencies between 0 and 1), calibrated on the Milky Way Galaxy (MWG). SF was assumed to occur in two steps: 1) molecular clouds forming from diffuse gas; 2) cloud-cloud collisions creating stars. Radial distributions for **both** gas phases were derived, but the inferred predicted ratios of atomic to molecular gas, and SF rate (SFR), were found to be at variance with those observed. We are computing a new grid of models with updated stellar yields –Mollá et al. (2015)–, gas infall rates –Mollá et al. (2016a)–, and molecular gas formation efficiency –Mollá et al. (2016b). Our aim is to improve the predicted H_2 and SFR profiles, while maintaining abundance radial gradients in agreement with those observed. We summarize our updated models and results in §2 and our conclusions in §3.

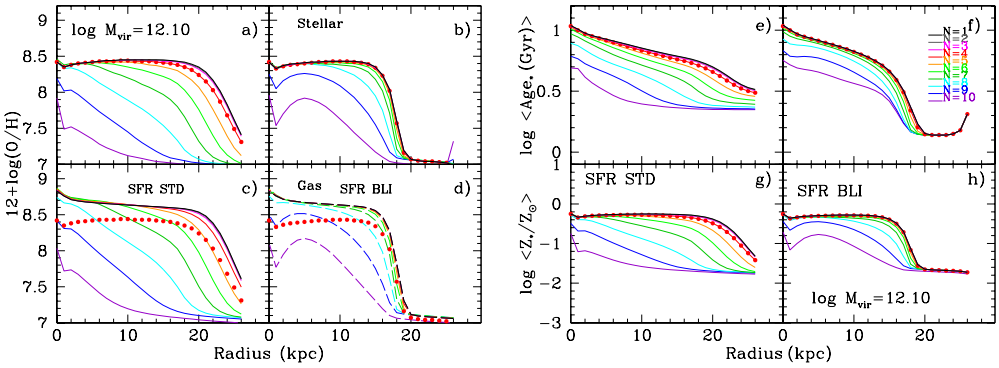

Figure 1. Radial distributions of oxygen abundances for stars (panels a and b) and gas (panels c and d) obtained with STD (panels a and c) and BLI models (panels b and d). Radial distributions of stellar average age, in logarithmic scale in e) and f); and averaged metallicity, $< Z/Z_{\odot} >$, in g) and h), obtained with STD, e) and g) and BLI, f) and h), models. Each color shows a different SF efficiency value. See text for more explanations.

2. New chemical evolution models

As described in Mollá et al. (2016a), we compute the radial mass distributions for 16 theoretical galaxies, following Salucci et al. (2007), who define them in terms of M_{vir} and their associated rotation curves. The virial masses, defined as the total dynamical mass for a galaxy, are in the range $M_{vir} \in [5 \times 10^{10} - 10^{13}]\, M_{\odot}$, with associated disk masses in the range $M_{disk} \in [1.25 \times 10^{8} - 5.3 \times 10^{11}]\, M_{\odot}$. The initial gas in each model collapses onto the disk on timescales based in Shankar et al. (2006), which gives the ratio between the disk and the virial masses, M_{disk}/M_{vir}. From the rotation curves, we calculate the radial distribution of the dynamical mass and the one that the disk will have at the present time. Thus, we obtain the infall rate necessary to have, at the end of a model's evolution, the appropriate disk for each dynamical mass. The inferred infall rates evolve modestly with time for the disks (stronger for bulges), showing, among radial regions or among galaxies, only variations in the absolute values. The radial regions in a disk for a galaxy with $M_{vir} \sim 10^{12}\ M_{\odot}$ (i.e., a MWG-like analog), have infall rates at the present time $\dot{M} \sim 0.5\, M_{\odot}\, yr^{-1}$ for galactocentric radii $R < 13\,$kpc, in agreement with Sancisi et al. (2008)'s data, while it is much lower in the outer regions ($R > 13\,$kpc).

By following Mollá et al. (2015), we use the stellar yield sets from Limongi & Chieffi (2003), Chieffi & Limongi (2004) for massive stars combined with the IMF from Kroupa (2001), joined to yields from Gavilán, Buell, & Mollá (2005), Gavilán, Mollá, & Buell (2006) for the low and intermediate mass stars.

Molecular gas in our models is created from diffuse gas. The efficiency of this process takes a value between 0 and 1, as a probability factor, in our standard models (STD), with an exponential function: $\epsilon_c = exp(N^2/20)$. With $N = 4$ we obtain a MWG-like model that produces a good fit for the evolution of the solar region, and for the radial distributions of gas, stars, SFR, and elemental abundances of C, N, and O, as shown in Mollá et al. (2015). We now check, in Mollá et al. (2016b), the prescriptions in creating molecular gas from Fu et al. (2010), based upon Blitz & Rosolowsky (2006): the H_2 fraction depends on total pressure, which, in turn, depends on gas and stellar surface densities. This model (BLI) is contrasted with STD. The dependence on stellar density produces a threshold effect, and in this way the evolution is slow at the beginning, but stronger at later times in the BLI model, relative to the STD. This produces a steepening of the radial distributions: the gradients of oxygen in stars and gas, $12+log(O/H)$, stellar

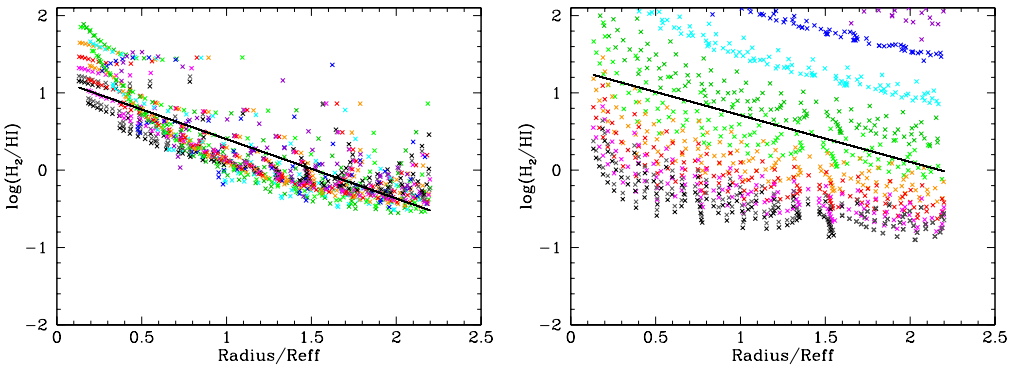

Figure 2. The ratio HI/H_2 versus the normalized radius R/R_{eff}, for the 76 galaxy models and 10 values of efficiencies to form stars in the: left) STD; right) BLI models.

age log $< Age >$ (Gyr), and metallicity $< Z/Z_{\odot} >$ are steeper in the BLI panels (b,d,f,h), with a strong flattening in the outer disk, compared with the STD results (even showing a U-shape in age in the outermost regions, in the absence of any stellar radial migration) at the last radial region). Finally, we show in Fig. 2, the normalized radial distribution of the molecular gas fraction obtained for our new models, using the STD and BLI options, compared with the empirical relationship obtained from Bigiel et al. (2008). The BLI models, while showing reasonable global trends, do not fit the data well.

3. Conclusions

• A grid of chemical evolution models with 16 dynamical masses in the range 10^{10} to $10^{13}\,M_{\odot}$ is calculated. A MWG-like model reproduces very well the observed radial distributions, as shown in Mollá et al. (2015) and Mollá et al. (2016b).

• Prescriptions from Blitz & Rosolowsky (2006) and Fu et al. (2010) for the formation of H_2 (BLI models) produce radial variations in O, $< Age >$, and $< Z/Z_{\odot} >$ which are stronger than STD models. Radial gradients are shown to be not invariant with radius.

• The H_2/HI relationship from Bigiel et al. (2008) is obtained for STD models, while BLI shows an unrealistically high dispersion.

References

Bigiel, F., Leroy, A., Walter, F., et al. 2008, *AJ*, 136, 2846
Blitz, L., & Rosolowsky, E. 2006, *ApJ*, 650, 933
Chieffi A., Limongi M. 2004, *ApJ*, 608, 405
Fu, J., Guo, Q., Kauffmann, G., & Krumholz, M. R. 2010, *MNRAS*, 409, 515
Gavilán M., Buell J. F., Mollá M. 2005, *A&A*, 432, 861
Gavilán M., Mollá M., Buell J. F. 2006, *A&A*, 450, 509
Kroupa P. 2001, *MNRAS*, 322, 231
Limongi M., Chieffi A. 2003, *ApJ*, 592, 404
Mollá M., Díaz A. I. 2005, *MNRAS*, 358, 521
Mollá, M., Cavichia, O., Gavilán, M., & Gibson, B. K. 2015, *MNRAS*, 451, 3693
Mollá, M., Díaz A. I., Gibson, B. K., et al. 2016a, *MNRAS*, in press
Mollá, M., Ascasibar, Y., Gibson, B. K., & Cavichia ,O. 2016b, *MNRAS*, to be submitted
Salucci P., Lapi A., Tonini C., Gentile G., Yegorova I., Klein U., 2007, *MNRAS*, 378, 41
Sancisi, R., Fraternali, F., Oosterloo, T., & van der Hulst , T. 2008, *A&ARv*, 15, 189
Shankar F., Lapi A., Salucci P., De Zotti G., Danese L. 2006, *ApJ*, 643, 14